

## Design and experimental verification of a new type of cutter for shield machine cutting underground plastic drainage boards

Qiuping Wang<sup>1,2</sup> , Wanli Li<sup>1</sup>, Zhikuan Xu<sup>1</sup> , Yougang Sun<sup>3</sup> 

<sup>1</sup>Tongji University, School of Mechanical Engineering, Shanghai, China.

<sup>2</sup>Shanghai Urban Construction Tunneling Equipment Co., Ltd., Equipment Design and Research Institute, Shanghai, China.

<sup>3</sup>Tongji University, Institute of Rail Transit, Shanghai, China.

e-mail: wangqiuping@stecmc.com, cnlwl@tongji.edu.cn, zhikuanxu@tongji.edu.cn, 1989yoga@tongji.edu.cn

### ABSTRACT

The construction of shield machines will confront complex geological types, to solve the safety problem caused by the material toughness of plastic drainage boards (also known as PVD) during shield tunneling, a new type of shield machine cutter for breaking plastic drainage board is proposed in this paper. Firstly, a mechanical model of the interaction between the cutter and the material is established, calculation analysis and comparison are carried out. Then, the cutting ability of the new cutter on drainage board under different conditions is tested, and corresponding experimental data are obtained, verifying the advantage of the new cutter proposed in this paper. The finite element analysis software LS-DYNA is used for simulation and based on a plastic drainage board cutting project in Singapore, an experiment platform for shield machine cutter to break plastic drainage board is designed to conduct experiments. This work will provide technical guidance for the material cutting engineering of actual drainage boards.

**Keywords:** Shield machine; Plastic drainage board; Prefabricated vertical drain (PVD); Cutter design.

### 1. INTRODUCTION

When carrying out underground construction, it is necessary to consider the physical and chemical properties of the strata [1]. Shield machines are widely used in the construction projects such as subways and tunnels because of the high mechanization degree, insensitive to environmental factors, and adaptability to different geological conditions [2]. When constructing shield machines in different geological strata, it is necessary to choose appropriate cutter and layout forms, factors such as soil type, rock hardness, and water content need to be considered [3]. The excavation efficiency and cutter wear of shield machines under different construction conditions have always been a research focus, especially for the excavation safety in complex geology with ductile materials, which is a challenge [4].

The construction of shield machines will confront complex geological types, and researchers have proposed methods for dealing with different strata with various cutters. GENG *et al.* [5] analyzed the shortcomings of traditional finite element simulation of shield machine rock breaking with disc cutters, simulated rock cutting models with four different material definition strategies, the results showed that the rock breaking process under the blade tip and the differences in tensile and compressive strength of rock should be considered as important factors. GUO *et al.* [6] collected thrust, torque, and rotational speed of the cutterhead during shield tunneling in complex strata, analyzed these parameters using mathematical statistical analysis methods and proposed optimization suggestions for excavation parameters. ZHU *et al.* [7] conducted tunnel excavation model experiments, revealing the effects of tunnel depth, cutterhead opening rate, and driving speed on thrust and torque, providing guidance for the construction of shield machine on soft soil foundations. FANG *et al.* [8] conducted a series of simulations using a coupled model considering the interaction between the cutters and the stratum, analyzing the effects of penetration depth, linear velocity, and wear on the performance of the cutter. LIN *et al.* [9] conducted rock cutting wear tests, revealing the effects of load, vibration, rock properties, and wear mechanisms on the wear. XIA *et al.* [10] optimized the structural parameters of the shield machine scraper and successfully applied the optimization results to a tunnel project. DUAN *et al.* [11] studied the influence of shield machine cutter shape on rock cutting performance and found that round end cutters have better rock breaking effects. The above research mainly focuses on the material wear characteristics and excavation efficiency of shield machine

cutters in natural strata such as hard rock, soft rock, and soft soil, there is still a lack of research on the treatment of underground artificial remnants by shield machine cutters.

At present, the process of cutter design mainly includes structural design, simulation calculation, experimental analysis, parameter optimization, and comparative evaluation indicators. WANG *et al.* [12] proposed a point grinding method for designing circular tooth cutting tools on curved surfaces, and conducted cutter manufacturing and gear slicing experiments to verify the effectiveness of the proposed cutter design and manufacturing method. NAIZABEKOV *et al.* [13] studied the mechanical properties of austenitic stainless steel after multiple radial shear rolling, providing a reference for cutter material selection. DU *et al.* [14] used 3D printing technology to manufacture four cricket tooth like cutters, designed experiments, and studied their performance in cutting force and energy, providing a reference for designing efficient tea tree harvesters. FARROKH [15] proposed an optimization method for shield machine cutters, which reveals the optimal spacing of disc cutters and their corresponding inclination angle, as well as the normal force of peripheral cutters. CHENG *et al.* [16] optimized the geometric parameters of the cutter from the aspects of cutter structure, disc diameter, and cutter tooth density, and verified the performance of the optimized cutter through two-level fuzzy comprehensive evaluation. MOMIN *et al.* [17] conducted sugarcane harvesting experiments using four types of cutters, analyzed cutting quality indicators and blade wear indicators, and summarized the impact of each blade on sugarcane harvesting quality. The above analysis shows that the contribution of existing research mainly focuses on cutter design and optimization, but there is still a lack of research on cutter design for shield machines, especially the lack of cutter design methods suitable for complex geological environments with ductile materials.

In practical engineering, plastic drainage boards (also known as PVD), as the main underground artificial remnants, have typical characteristics of ductile materials, which pose great challenges to the safety of shield tunneling construction [18]. At present, research on plastic drainage boards cutting mainly focuses on theoretical analysis and simulation, and the research on new cutter design and experimental verification is not deep enough [19]. To solve the problem of shield machine excavation in complex geology with PVD, this paper studies the material properties of PVD and proposes a new type of PVD cutter, the force changes during the cutting process are studied through finite element simulation, and compared with existing cutters used in engineering to cut PVD, finally, an experimental platform is built to study the actual cutting mechanism.

## 2. BACKGROUND OF PVD

The drainage board consolidation method is one of the commonly used methods in soft foundation treatment of ground engineering [20]. As shown in Figure 1, prefabricated vertical drain (PVD) is a kind of strip material with a core made of plastic, grooves on both sides, and wrapped in geotextile, other parameters are detailed in Table 1. The plastic drainage boards are mainly composed of high-density polypropylene and polyethylene, with a density of about  $1.2 \text{ g/cm}^3$  and a tensile strength between 20 and 40 MPa. They have good heat and cold resistance and can be used at temperatures ranging from  $-30$  to  $140 \text{ }^\circ\text{C}$ . It has a width of about 10 cm and a thickness of about 4 mm, during construction, plastic drainage boards are arranged in a triangular pattern at a distance of about 1 m, they are inserted into soft soil using a spile machine, with a maximum depth of about 35 m underground, under the upper preloading load, the pore water in the soft soil foundation is discharged through PVD, accelerating the consolidation process of the soft soil and improving its strength and stiffness [21].

With the development of urban rail transit, subway tunnels constructed with shield machine inevitably need to cross soft soil strata. Prefabricated vertical drain, as waste left in the soil during the process of soft soil foundations, have the characteristics of being difficult to degrade, corrosion-resistant, and good toughness [22–24].

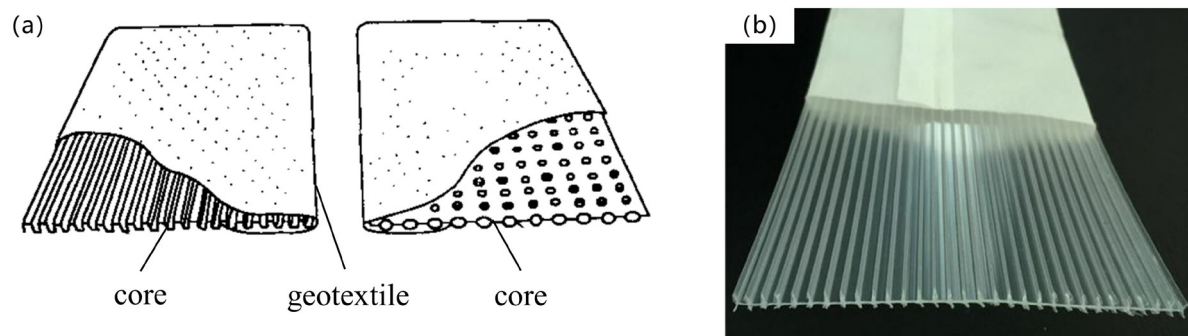


**Figure 1:** (a) Sketch map of PVD; (b) physical image of PVD.

**Table 1:** Performance indicators of PVD.

ITEM		TYPE				
		A	A0	B	B0	C
Applicable drilling depth, m		10	15	20	25	35
Thickness, mm		≥3.5	≥3.5	≥4.0	≥4.0	≥4.5
Material	Core	High density polyethylene, polypropylene, etc.				
	Filter membrane	Polyester and polypropylene; Mass per unit area > 85 g/m <sup>2</sup>				
Complex	Tensile strength (dry state), kN/10 cm (strength with an elongation of 10%)	>1.0	>1.0	>1.2	>1.2	>1.5
	Elongation, %	>4				
Tensile strength, kN/m	Dry tensile strength	1.5	1.5	2.5	2.5	3.0
	Wet tensile strength	1.0	1.0	2.0	2.0	2.5
Core plate flexural strength, kPa		>250			>350	

When shield machines pass through areas with plastic drainage boards, possible situations include: (1) Long plastic drainage boards will wrap around cutterhead and cutters, reducing the excavation speed; (2) The cut-off plastic drainage board will be wound into ball in the shield machine's soil bin, piled up in an arch shape, blocking the soil inlet of the screw conveyor, resulting in the inability to discharge soil. These pose a great risk to tunnel construction and if not handled properly, it may lead to the shield tunneling machine being trapped and causing personnel and property damage [25].

In theory, the removal of drainage boards can be achieved through methods such as high-temperature melting, freezing, chemical corrosion, and direct cutting of shield machine. When using the high-temperature melting method, the high-temperature resistance of the drainage plate in tunnel construction is around 120 °C, while the maximum temperature that the shield tunnel seal can withstand is 80 °C, this method can easily lead to the failure of the shield tunnel seal. When using the freezing method, the drainage plate does not crack at -35 °C and only becomes brittle, while the shield sealing is prone to failure at low temperatures, and the cutterhead shield may be trapped due to soil freezing. The use of chemical corrosion can degrade the drainage board, but injection is difficult and the dosage is difficult to control. Therefore, by comprehensive comparison, using shield machine cutters to directly break through is the most feasible and minimally influential method.

### 3. DESIGN OF PVD CUTTER

This section will analyze some plastic drainage board cutting projects, summarize the characteristics of cutters with excellent cutting effects, and based on this, design tools specifically for cutting PVD.

In a project in Zhuhai, Shanghai Tunnel Engineering Co., Ltd. used non sharp edged cutters such as the ripper (Figure 2a) and the claw cutter (Figure 2b), PVD cutting tests showed that the length of drainage debris was too large (Figure 3), mostly broken by pulling, and the longer drainage plate also caused blockage of the muddy water tank (Figure 4). A welding sharp edge tear cutter was designed based on conventional tooth cutters in a project in Ningbo (Figure 2c), based on the research of experimental and construction results, when using conventional tooth cutters and serrated tooth cutters to damage the drainage board, the incision of the drainage board is not neat, which clearly belongs to tensile stress damage (Figure 5). When using the welding sharp edge tear cutter to damage the drainage board, the incision of the drainage board is regular and belongs to a typical shear cutting (Figure 6), in which case the chips on the drainage board are shorter [26].

Given the several cutting results shown in Figures 3 to 6, this paper proposes a new type of PVD cutter to meet the excavation requirements in complex geology with plastic drainage boards.

Since the strata to be crossed are soil layers and drainage boards, the main purpose is to improve the cutting rate of the drainage board, therefore, the cutting edge of the cutter adopts an acute angle design to improve the cutting ability, the cutting area of the cutter body is wider than that of the blade, which can improve the impact resistance and durability. Meanwhile, the cutter is double edged designed to facilitate the forward and reverse collaborative operation of the cutterhead, the cutter design is shown in Figure 7, hereinafter referred to as PVD cutter.

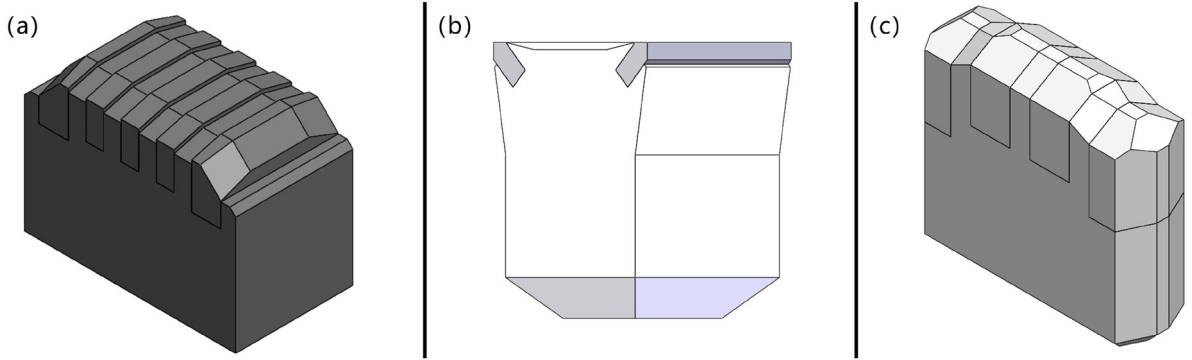


**Figure 2:** (a) Ripper, (b) claw cutter, (c) tear cutter.



**Figure 3:** Cutting chips from PVD with ripper.



**Figure 4:** PVD blockage of sludge tank.

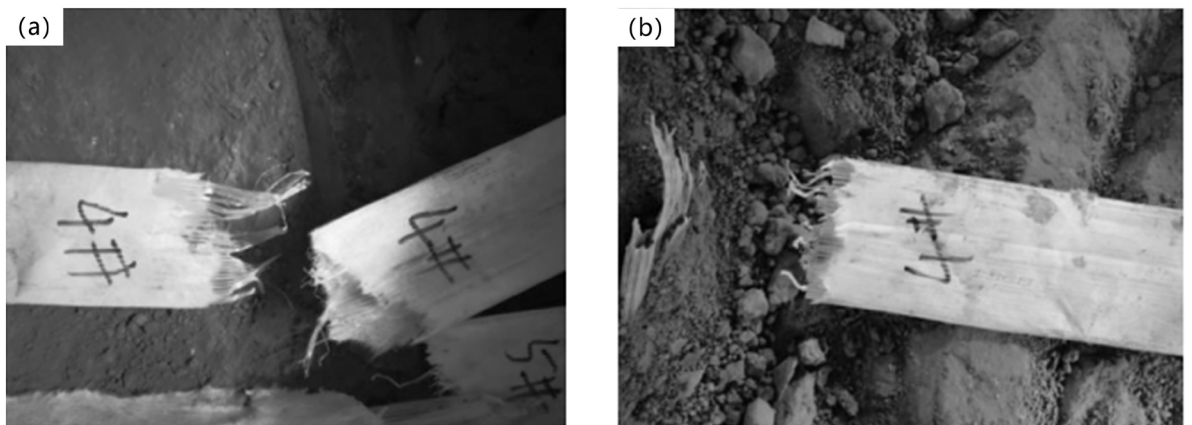


**Figure 5:** The fracture state of conventional and serrated blade cutting PVD.

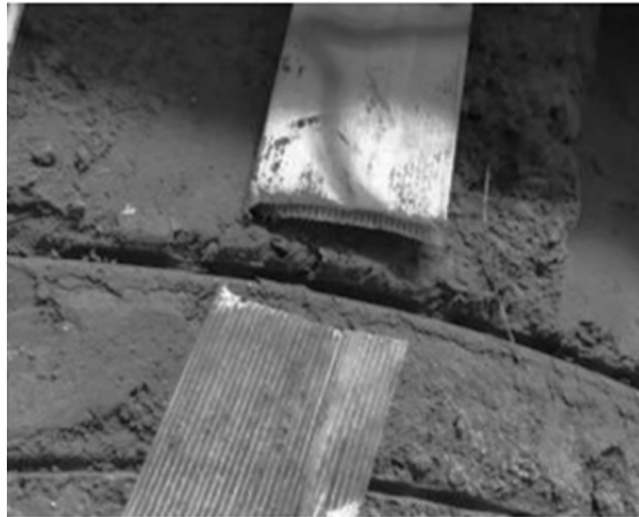


Figure 6: Tear cutter cutting PVD fracture state.

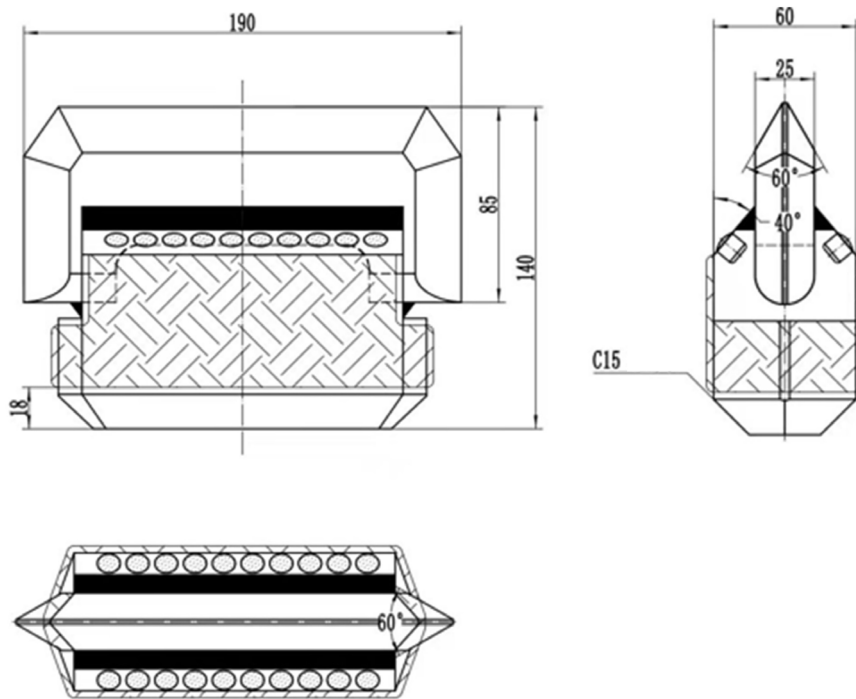


Figure 7: PVD cutter.

The size and shape of cutter are mainly based on actual needs and wear life theory. The width of the plastic drainage board is 100 mm, to ensure the cutting effect, the cutter width is designed to be approximately twice that of it, which is 190 mm. The cutter not only rotates clockwise and counterclockwise on the cutterhead, but also feeds along the axial direction, the feed rate per revolution is usually 10–40 mm, so the height of the cutter body is designed to be 40 mm. The thickness of the blade body considers the theory of wear life, and the specific life design calculation is as follows:

$$L = 10000 \frac{P_e t}{2\pi R k} \tag{1}$$

Where:

$L$  = Distance that can be excavated when reaching the cutter wear limit.

$k$  = Wear coefficient of cutter.

$t$  = The allowable wear thickness of cutter.

$R$  = The installation radius of the outermost cutter.

$P_e$  = The cutting depth per revolution.

Considering that the working distance the cutter needs to meet is 220 m, the maximum excavation distance designed based on twice the service life is 440 m. By substituting the cutter parameters and the correlation coefficient during construction into Equation 1, it can be inferred that the thickness of the cutter that meets the design life is approximately 25 mm.

The cutter blade is made of T11 die steel into C-double-blade type and coated on the surface to make it have good wear resistance. The cutter body is made of Q345 low-alloy high-strength structural steel with high strength and good weldability, and 3~5 mm wear-resistant layer on its surface had a hardness of HRC58~60, which can effectively ensure that the cutter head is subjected to long-term wear without damage. After the blade is manufactured, it is inserted into the groove of the cutter body and welded firmly through the silver base brazing technology. Then the cutter body with blade is welded to the installation holder through 15 mm chamfer at the bottom to become a complete PVD cutter, as shown in Figure 8. The cutter shaft on the holder is same as the shaft of the disc-cutter so that they can be interchanged on the cutter head.

#### 4. MECHANICAL MODEL OF THE INTERACTION BETWEEN CUTTER AND MATERIAL

In order to verify the superiority of the proposed PVD cutter, simulation models for cutting PVD with different cutters will be established to simulate the process of cutting PVD, and comparative analysis of the cutting performance of ductile materials with different cutters is carried out.

Firstly, establish a three-dimensional model of the PVD and the cutter, considering the convenience of modeling and shortening the calculation time of subsequent simulations, simplify the model without affecting the calculation accuracy, consider the cutter as a rigid body and simplify the PVD with grooves on both sides into a smooth horizontal plate, with a thickness of 4 mm, a width of 100 mm, and a length of 500 mm. Then mesh the model, treating PVD as composed of shell elements and cutters as composed of rigid body elements, and increasing the mesh density of the cutter tip while reducing the mesh density of the remaining parts. Next, define the material parameters, the selected parameters are the general and mechanical properties of materials used in finite element analysis, the cutter material is uniformly defined as Q345 steel, the mechanical properties are shown in Table 2, according to the Chinese national standard «Geosynthetics in highway engineering-Plastic drainboard» and Liu and Chu's research on the physical properties of plastic drainage boards, the mechanical properties of PVD are defined as shown in Table 3 [27].

In engineering, the actual circular motion of the cutter is usually around 1 r/min, but its motion radius is much larger than the size of the drainage board and cutter. Therefore, the motion of the cutter can be approximated as a linear motion with a speed of about 150 mm/s.

Referring to the arrangement of cutters on the cutterhead of the shield machine, as shown in Figure 9, simulation experiments for cutting drainage boards with different cutters can be design. As shown in Figure 10, a coordinate system is established with the cutter as a reference, the cutting direction is defined as the Z-axis,



**Figure 8:** Installed PVD cutter.

**Table 2:** Mechanical properties of cutter.

	DENSITY(kg/m <sup>3</sup> )	ELASTIC MODULUS (GPa)	POISSON'S RATIO
Cutter	7850	200	0.3

**Table 3:** Mechanical properties of PVD.

	DENSITY (kg/m <sup>3</sup> )	ELASTIC MODULUS (GPa)	POISSON'S RATIO	YIELD STRENGTH (MPa)	TENSILE STRENGTH (MPa)	FAILURE STRAIN
PVD	1200	0.9	0.42	22	29	10%

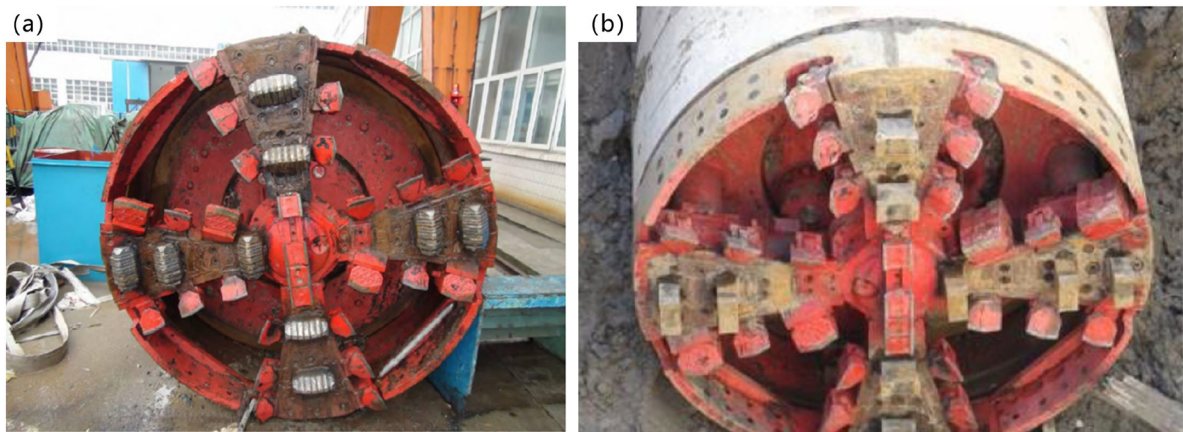


**Figure 9:** (a) Cutterhead with ripper; (b) cutterhead with claw cutter.

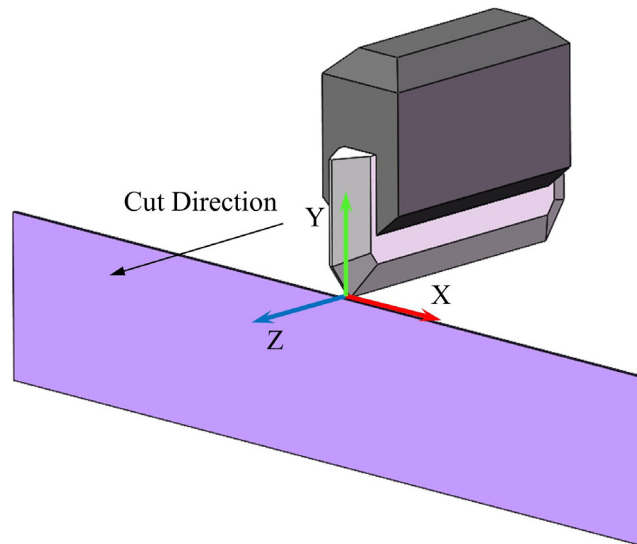


**Figure 10:** Experimental design.

the direction perpendicular to the cutter side is defined as the X-axis, and the normal vector direction of the XZ plane is defined as the Y-axis, the drainage plate is placed parallel to the XY plane, and the lowest point of the cutter is 25 mm below the upper edge of the drainage plate, the cutter cuts the drainage plate at a speed of 150 mm/s, and the force situation of different cutters and the cutting status of the drainage plate are recorded and analyzed.

### 5. NUMERICAL SIMULATION CALCULATION OF CUTTING PROCESS

The four types of cutters cutting PVD simulation calculations result is shown in Figure 11. It can be seen that the cutting surface of the PVD cutter is relatively neat, with obvious notches on the PVD, while the notches of the other cutters are tear and pull type failures.

Studying the resultant force on the cutter during the simulation process, it can be found that the period of cutting PVD is from the sudden change in force to the force falling back to 0, as shown in Figure 12. It can be clearly seen that the PVD cutter proposed in this paper has a smaller maximum force and the shortest cutting period compared to other cutters, which means having advantages in cutting PVD.

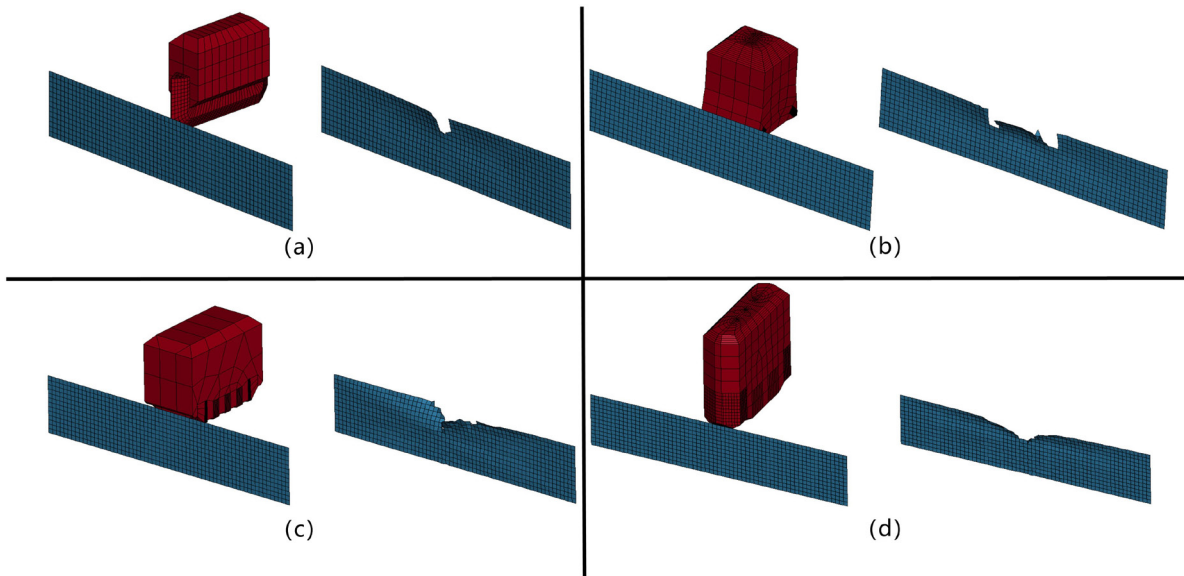


Figure 11: (a) PVD cutter, (b) claw cutter, (c) ripper, (d) tear cutter.

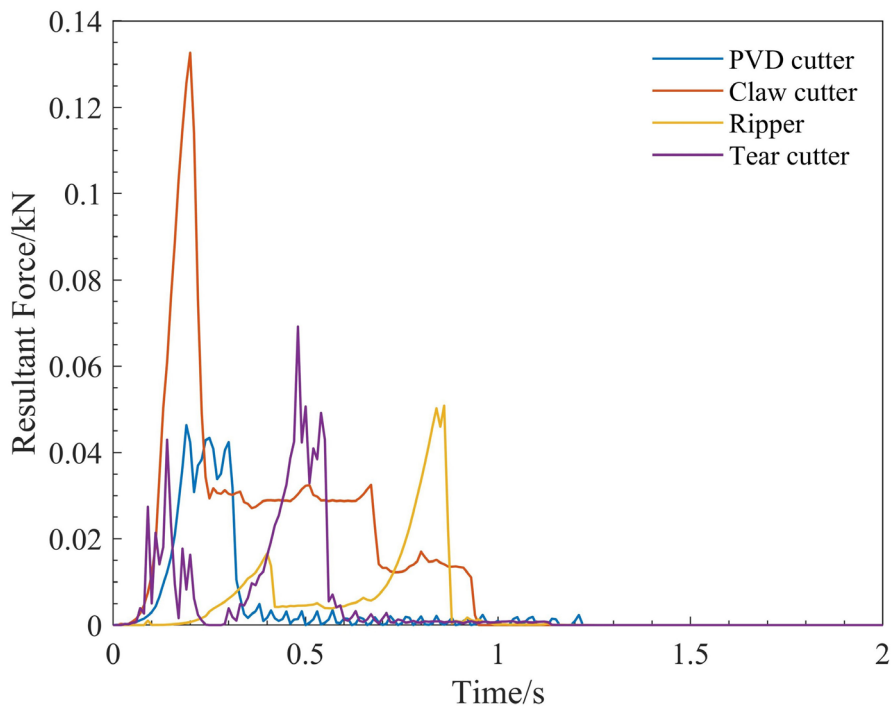


Figure 12: Cutter force diagram.

## 6. EXPERIMENTATION

On the basis of sufficient simulation research, build an experimental platform and conduct on-site cutting experiments to verify the cutting effectiveness of the proposed PVD cutter.

### 6.1. Experimental platform

A linear cutting device (shaping machine) was used for single blade cutting experiments, as shown in Figure 13, the cutting device is mainly composed of machine bed, ram, workbench, blade carrier, etc. The machine bed is mainly used to support and connect the relevant components of the machine. The ram moves back and forth through the slide rail on the top surface of the machine bed. The blade carrier serves as the carrier for cutters and is located in front of the ram. The workbench is used to place test samples, which can be adjusted up and down, and can move horizontally along the crossbeam guide rail. There are two speed controller, the two controller work together to complete the control of cutting speed.

### 6.2. Monitoring equipment

The data acquisition system adopts FC3D sensors, as shown in Figure 14, FC3D is a miniature high precision triaxial force sensor that can simultaneously test the force values in  $x$ ,  $y$ , and  $z$  directions, it is widely used in detection equipment such as vehicle engineering, biomedicine, and artificial intelligence. The main body of the sensor is made of 40CrMo alloy steel, and the sealing material is made of silicone rubber, which has excellent corrosion resistance and a compact overall structure.

The sensor is placed between the blade carrier and the top plate of the cutting device to complete real-time collection of cutting force, after being processed by an amplifier, the output signal is collected and displayed in real-time through a multi-channel data collector in the matching FC-DAQ multi-channel data acquisition software, the multi-channel data collector can collect up to six sensor data simultaneously and display them in the acquisition software, only one of them was used in this experiment, the specific flowchart is shown in Figure 15.



Figure 13: Linear cutting test device.



Figure 14: Triaxial force sensors.

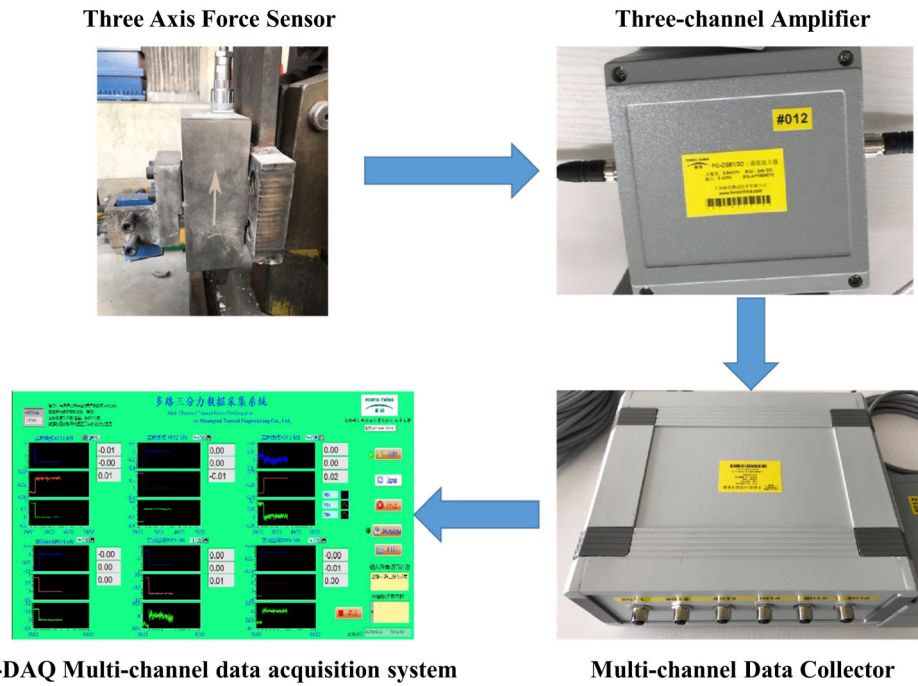


Figure 15: Collection process.

Table 4: Technical parameters related to triaxial force sensors.

SENSITIVITY/(MV/V)	NONLINEAR ERROR	HYSTERESIS ERROR	UNIDIRECTIONAL COMPREHENSIVE ERROR	PERMITTED OVERLOAD
0.5~1.5	<0.15%	<0.25%	<0.3%	120%

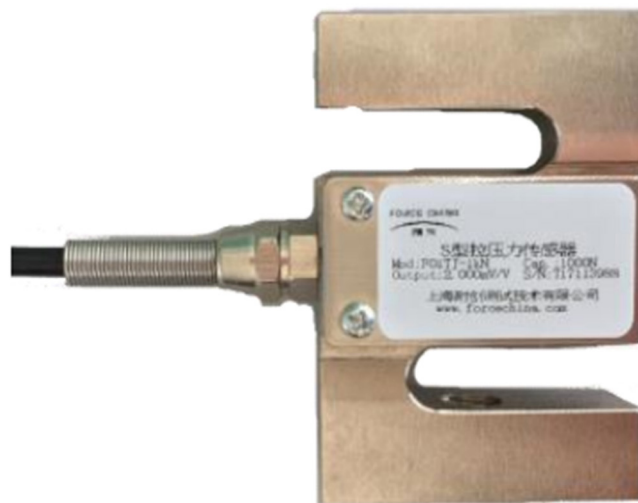


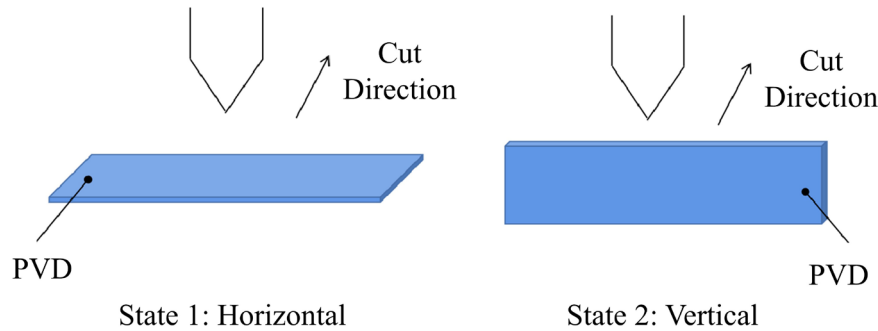
Figure 16: S-type tension sensor.

The selection of sensor range is based on simulation research results, the range of the X, Y, and Z axes of the sensor is 10 kN, and other related parameters are shown in Table 4.

The auxiliary device adopts an S-type tension sensor (Figure 16) with a sensor range of 7 kN, and the relevant parameters are shown in Table 5. Based on the experience of cutting drainage boards, the main failure

**Table 5:** Technical parameters related to S-type tension sensor.

SENSITIVITY/(MV/V)	NONLINEAR ERROR	HYSTERESIS ERROR	REPEATABILITY ERROR	PERMITTED OVERLOAD
2.0	0.1%F.S	0.1%F.S	0.05%F.S	150%

**Figure 17:** Two cutting states.**Table 6:** Cutting conditions.

CONDITION	PVD STATES	EXPERIMENT METHOD	NUMBER OF PVD LAYERS	CUTTING DEPTH	CUTTING SPEED
A1	State 1	Fix the PVD on both sides, Bottom suspended	1	5 mm	150 mm/s
A2	State 1	Fix the PVD on both sides, Bottom suspended	1	10 mm	150 mm/s
B1	State 2	Fix the PVD on both sides	1	5 mm	150 mm/s
B2	State 2	Fix the PVD on both sides	1	10 mm	150 mm/s
B3	State 2	Fix the PVD on both sides	1	15 mm	150 mm/s
B4	State 2	Fix the PVD on both sides	1	20 mm	150 mm/s
B5	State 2	Fix the PVD on both sides	1	25 mm	150 mm/s
B6	State 2	Fix the PVD on both sides	1	30 mm	150 mm/s

modes of drainage boards are expected to present three main states: (1) Complete cutting failure; (2) Rupture of the fixed side; (3) Chela damage. Therefore, the S-type tension sensor is installed on the fixed edge of the drainage board to record the tension when the fixed side of the drainage board is completely pulled apart.

### 6.3. Experimental conditions

The experiment was carried out without soil support and compression, which can be regarded as an infinitely soft soil. In practical engineering applications, the drainage board is surrounded by soil, which provides additional support and compression. The difficulty of cutting off the drainage board will be less than when it is suspended in the air. Therefore, model tests can be considered as the worst case. Because the cutting angle is between 0 and 90 degrees, the experiment mainly considers two extreme situations: horizontal and vertical.

For the cutting experiment of the drainage board, there are two placement states (Figure 17), and the cutting conditions are shown in Table 6. The experiment is mainly conducted from two perspectives: different placement forms of drainage boards and cutting depths. The test form with the bottom suspended is shown in Figure 18. The pedestal of the experimental platform can be adjusted in the  $z$ -direction, while the blade carrier can perform feed motion in the  $y$ -direction. The experimental process is as follows: first, fix the drainage board on the pedestal according to the required conditions, then move the blade above the drainage board, adjust the pedestal for cutter setting, then move the blade carrier back and raise the pedestal to a certain height, which is



Figure 18: Bottom suspended placement method.

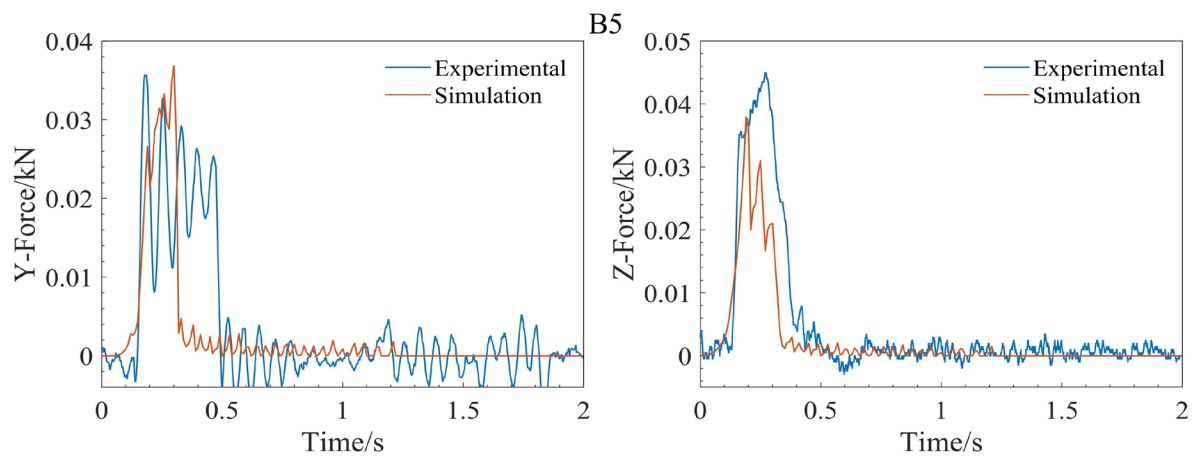


Figure 19: Experimental data and simulation data in B5.

equal to the required cutting depth. Then, start the machine and let the cutter repeatedly cut the drainage board five times, or stop when the drainage board is completely broken. Finally, record the experimental data and take the best quality data for analysis.

#### 6.4. Analysis of experiment results

Due to the toughness of the drainage board, it will deform when the cutting depth is not large under two conditions, leaving only inconspicuous cutting marks, which is also problem in practical engineering. Therefore, it is necessary to analyze the cutting force.

Cutting force is one of the important physical parameters in mechanical excavation, directly affecting the amount of power consumed and the wear rate of cutters during the cutting process. Analyzing and understanding the variation pattern of cutting force can help to make reasonable choices for the structural and construction parameters of cutters, effectively reduce cutter damage, and improve excavation efficiency.

This experiment collected forces in the  $x$ ,  $y$ , and  $z$  directions, where the  $x$  force is perpendicular to the side of the tool. The  $y$  force is perpendicular to the surface of the cutting material. The  $z$  force is along the cutting direction (as shown in Figure 10). During the experiment the cutting force on the drainage board is too small (less than 1 kN), based on actual test results it was found that the  $x$ -side force was so small that the force was even lower than the error fluctuation, therefore, the experimental results focused on studying the  $y$ -and  $z$ -direction forces.

Firstly, the experiment was conducted under the same B5 condition as the previous simulation, the simulation data was compared with the experimental data, and the results are shown in Figure 19, it can be seen that

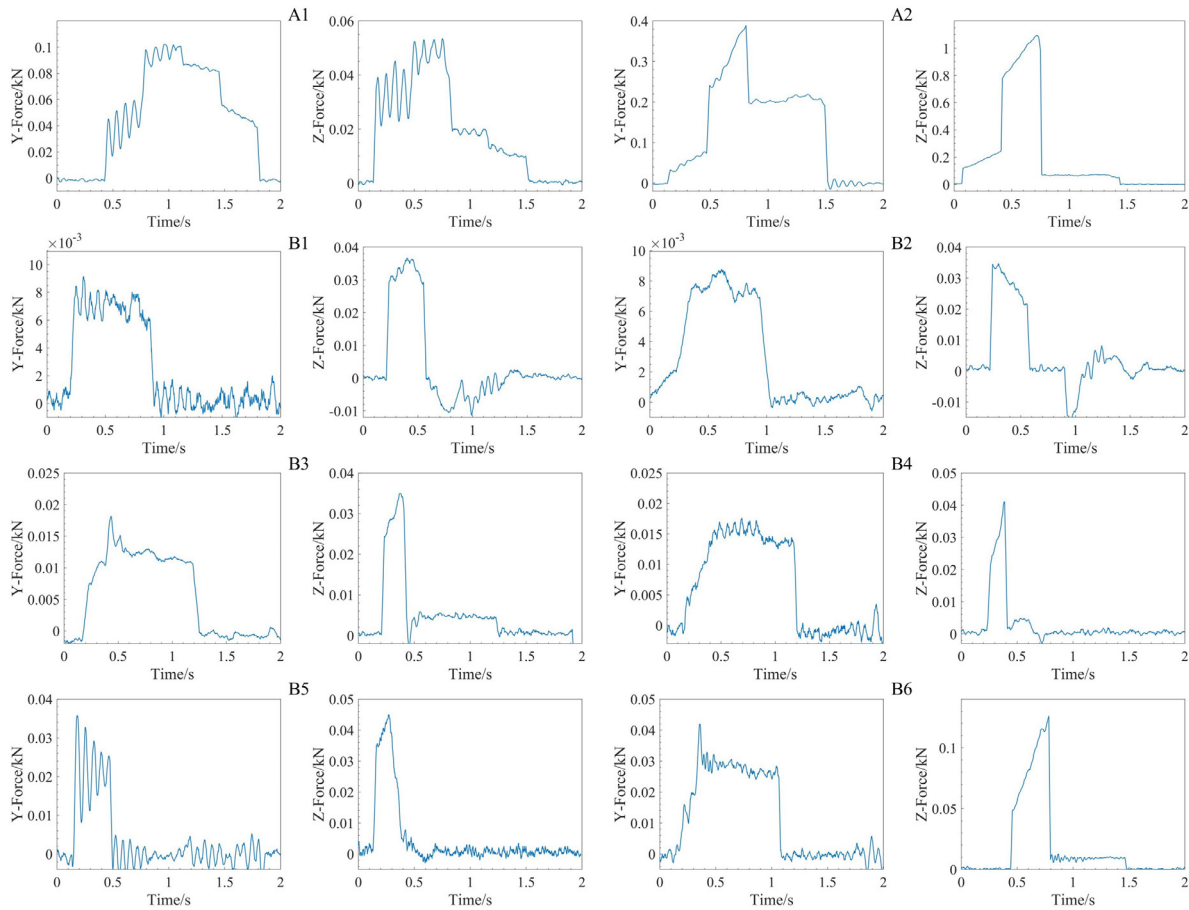


Figure 20: Experimental results.

the trend and peak values displayed by the experimental and simulation results are generally the same, which also proves the rationality of the established force model to a certain extent.

As shown in Figure 20, experimental data was recorded under other conditions and plotted as a graph. It can be observed that in condition A, by only increasing the cutting depth by 5 mm, the cutting force of A2 is much greater than that of A1. In condition B, as the cutting depth increases, the stable value of y-force will also increase, while the z-force does not show significant changes and exhibits the characteristic of pulse force.

In A1 condition, as shown in Figure 21b, it can be observed that the middle part shows obvious cuts, while the front and rear parts have scratches. Based on the experimental phenomenon, it can be inferred that the front part of the drainage board is subjected to the cutting force of the cutter, and the middle part is squeezed and raised. Due to the bottom of the drainage board being suspended, there is no adhesive force. When the middle of drainage board is raised to a height, it is forcibly torn open by the cutter thrust. Under continuous cutting, the drainage board in the middle part will be broken first. In actual cutting engineering, if the soil layer attached to the back end is peeled off first, such cutting situations will occur.

As shown in Figure 22, the drainage board easily fractures under A2 condition, this time the peak force in the z-direction of A2 condition is almost 20 times that of A1 condition. The larger z-direction impact force causes the drainage board to be directly pulled apart, but even the impact force of pulling apart still does not exceed 1 kN. When the tensile failure occurs, the lateral tensile force shows an increasing and then decreasing trend, with a final peak of 300 N.

By observing the cutting phenomenon in conditions A1 and A2, it can be found that in state 1, a significant proportion of drainage board fracture is caused by tensile failure. The common failure process is: cutter produces notches – continuous cutting results in tensile fractures – the proportion of tensile fractures increases – the drainage board breaks.

Experiments with a cutting depth of 5–30 mm are conducted in condition B, since the drainage board has no back support and is relatively soft compared to the cutter, the cutter mostly scratches over the drainage

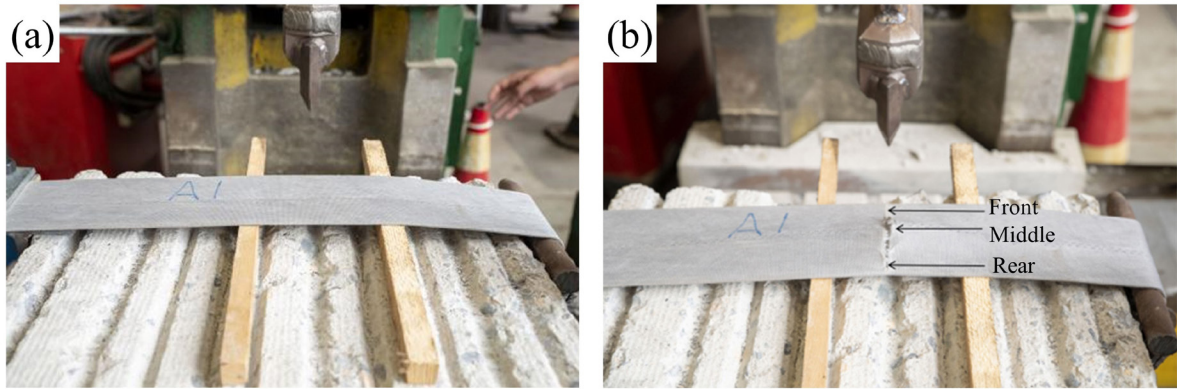


Figure 21: A1 condition cutting test (a) before, (b) after.

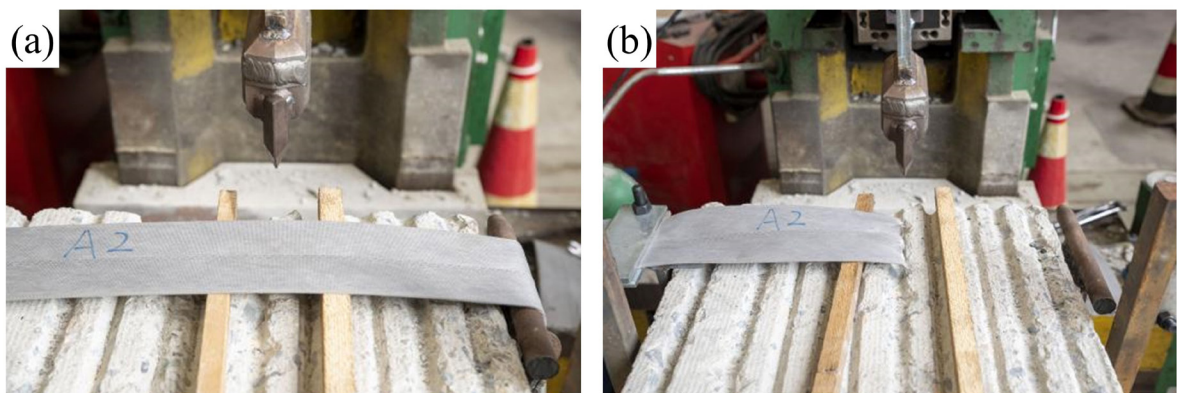


Figure 22: A2 condition cutting test (a) before, (b) after.

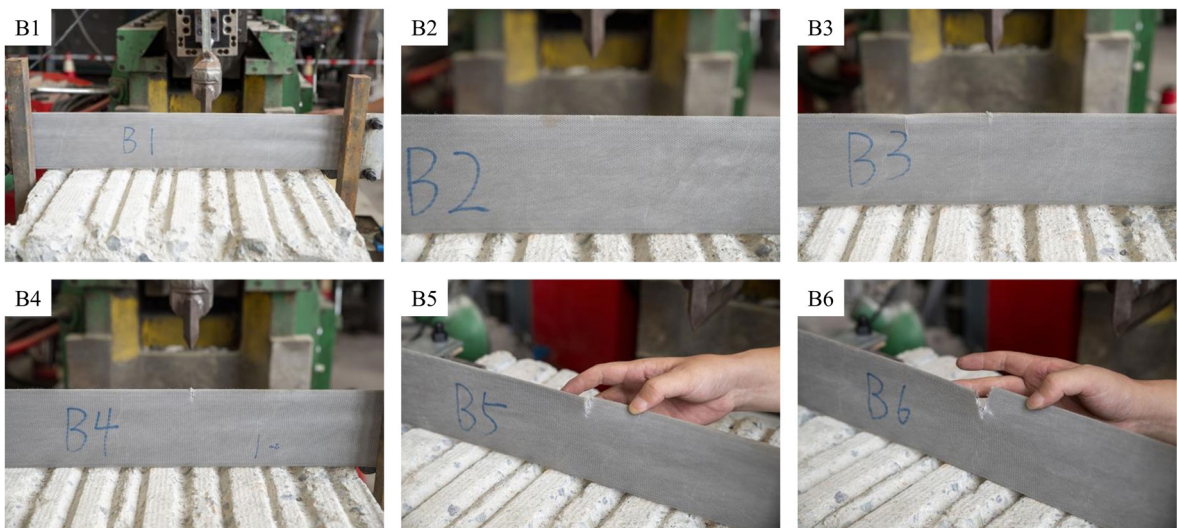


Figure 23: B condition cutting test.

board at a cutting depth of 5 mm and 10 mm, resulting in less obvious cuts. From the perspective of  $z$ -force, it mainly consists of two aspects: (1) The resistance of the cutter cutting the drainage board; (2) The resistance of the cutter scratching over the drainage board. When the cutter makes a cut on the drainage board, the resistance of the cutter passing through the drainage board remains basically the same, therefore, the peak of  $z$ -axis force indicates the resistance value of the cutter cutting the drainage board.

By comparing the  $z$ -axis forces at different cutting depths, it was found that cutting deeper did not result in a significant increase in the  $z$ -axis cutting force of the tool, meanwhile observing the incision of the drainage board in Figure 23, the incision appears as cut-off destruction. Therefore, it can be inferred that the cutter can effectively cut the drainage board in state 2, but it is necessary to avoid excessive cutting depth, as excessive cutting depth can cause the cutter to forcefully pull the drainage board through the cutter holder impact, thus losing the meaning of cutting.

By observing the cutting state under condition B, in state 2, the incision of the drainage board shows a cut-off destruction. If the cutting comes deeper, the drainage board will gradually be cut and damaged, or pulled apart when cutting to the end of the drainage board.

## 7. CONCLUSION

A cutter is designed specifically for cutting PVD on shield machines in this paper. Firstly, finite element analysis is used to compare other cutters used in engineering, proving that PVD cutter designed with sharp edges are more suitable for cutting drainage boards. Then, a PVD cutting experimental platform is designed and experiments are conducted to obtain three-dimensional force experimental data of the cutter under different conditions, it can be found that the PVD cutter proposed in this paper can perform good cutting on the drainage board in states 1 (drainage board horizontal) and 2 (drainage board vertical). The destruction process of state 1 is as follows: cutting produces an incision – continuous cutting produces a tensile fracture – the tensile fracture increases – the drainage board is pulled and damaged. The destruction process of state 2 is that the drainage board will gradually be cut off or pulled off at the end of the cutting port. The general cutting force in state 1 does not exceed 0.5 kN, and the  $z$ -direction force at fracture is 1.1 kN. The force variation of the cutter under different cutting depths in state 2 is relatively small, and all conditions do not exceed 0.05 kN.

The conventional cutters of shield machines may tear and damage plastic drainage boards, leaving long debris, the PVD cutter proposed in this article adopts an acute angle design and is double edged to meet the requirements of forward and reverse rotation of the cutting head, it can cut PVD into shorter fragments, meeting the cutting needs of ductile plastic drainage boards in complex geological conditions. Future research will focus on improving the universality of cutter, designing cutter that can cut other ductile materials, as well as cutter that can simultaneously cut hard, soft, and ductile materials.

## 8. ACKNOWLEDGMENTS

Authors are thankful to sponsorship by Shanghai Rising-Star Program (22QB1401900).

## 9. BIBLIOGRAPHY

- [1] SANTOS, L.M.A., SILVA NETO, J.A.D., AZERÊDO, A.F.N.D., “Soil characterization for adobe mixtures containing Portland cement as stabilizer”, *Matéria*, v. 25, n. 1, e12565, 2020. doi: <http://doi.org/10.1590/s1517-707620200001.0890>.
- [2] KASPER, T., MESCHKE, G., “A numerical study of the effect of soil and grout material properties and cover depth in shield tunnelling”, *Computers and Geotechnics*, v. 33, n. 4-5, pp. 234–247, 2006. doi: <http://doi.org/10.1016/j.compgeo.2006.04.004>.
- [3] TRIPATHI, B.N., AGRAWAL, A.K., RAY, D., *et al.*, “Expert system to select tunnel boring machine (TBM)”, *IOP Conference Series. Materials Science and Engineering*, v. 691, n. 1, pp. 012012, 2019. doi: <http://doi.org/10.1088/1757-899X/691/1/012012>.
- [4] WANG, H., ZHANG, M., SUN, R., *et al.*, “Performance improvement strategy of the TBM disc cutter ring material and evaluation of impact-sliding friction and wear performance”, *Wear*, v. 526–527, pp. 204943, 2023. doi: <http://doi.org/10.1016/j.wear.2023.204943>.
- [5] GENG, Q., WEI, Z., REN, J., “New rock material definition strategy for FEM simulation of the rock cutting process by TBM disc cutters”, *Tunnelling and Underground Space Technology*, v. 65, pp. 179–186, 2017. doi: <http://doi.org/10.1016/j.tust.2017.03.001>.
- [6] GUO, Z., ZHANG, H., SHI, X., *et al.*, “Research on shield tunnelling parameters correlation in composite strata”, *Advances in Materials Science and Engineering*, v. 2022, pp. 3973469, 2022. doi: <http://doi.org/10.1155/2022/3973469>.
- [7] ZHU, H., XU, Q., ZHENG, Q., *et al.*, “Experimental study on working parameters of earth pressure balance shield machine tunneling in soft ground”, *Frontiers of Architecture and Civil Engineering in China*, v. 2, n. 4, pp. 350–358, 2008. doi: <http://doi.org/10.1007/s11709-008-0051-5>.
- [8] FANG, Y., YAO, Z., XU, W., *et al.*, “The performance of TBM disc cutter in soft strata: A numerical simulation using the three-dimensional RBD-DEM coupled method”, *Engineering Failure Analysis*, v. 119, pp. 104996, 2021. doi: <http://doi.org/10.1016/j.engfailanal.2020.104996>.

- [9] LIN, L., XIA, Y., MAO, Q., *et al.*, “Experimental study on wear behaviors of TBM disc cutter ring in hard rock conditions”, *Tribology Transactions*, v. 61, n. 5, pp. 920–929, 2018. doi: <http://doi.org/10.1080/10402004.2018.1442895>.
- [10] XIA, Y., YANG, M., LIN, L., *et al.*, “Effect of blade angles on the shovel muck capacity and wear characteristics for TBM scraper”, *Arabian Journal for Science and Engineering*, v. 46, n. 5, pp. 5203–5218, 2021. doi: <http://doi.org/10.1007/s13369-021-05425-w>.
- [11] DUAN, W., ZHANG, L., ZHANG, M., *et al.*, “Numerical and experimental studies on the effects of the TBM cutter profile on rock cutting”, *KSCE Journal of Civil Engineering*, v. 26, n. 1, pp. 416–432, 2022. doi: <http://doi.org/10.1007/s12205-021-2111-5>.
- [12] WANG, P., HAN, L., LI, J., *et al.*, “Research on design and manufacturing of gear slicing cutter for circular arc tooth”, *International Journal of Advanced Manufacturing Technology*, v. 113, n. 7-8, pp. 2017–2029, 2021. doi: <http://doi.org/10.1007/s00170-021-06757-5>.
- [13] NAIZABEKOV, A., LEZHNEV, S., PANIN, E., *et al.*, “Realization of the innovative potential of radial-shear rolling for forming the structure and mechanical properties of AISI-321 austenitic stainless steel”, *Matéria*, v. 26, n. 3, e13018, 2021. doi: <http://doi.org/10.1590/s1517-707620210003.13018>.
- [14] DU, Z., HU, Y., LU, Y., *et al.*, “Design of structural parameters of cutters for tea harvest based on biomimetic methodology”, *Applied Bionics and Biomechanics*, v. 2021, pp. 8798299, 2021. doi: <http://doi.org/10.1155/2021/8798299>. PubMed PMID: 34335873.
- [15] FARROKH, E., “Optimum design of the peripheral cutters’ specification on the head profile for hard-rock TBMs”, *Tunnelling and Underground Space Technology*, v. 107, pp. 103668, 2021. doi: <http://doi.org/10.1016/j.tust.2020.103668>.
- [16] CHENG, Y., JIA, W., NIE, W., *et al.*, “Optimum design and performance evaluation of layer face milling cutter for cutting 508III steel”, *International Journal of Advanced Manufacturing Technology*, v. 98, n. 1–4, pp. 729–740, 2018. doi: <http://doi.org/10.1007/s00170-018-2272-7>.
- [17] MOMIN, M.A., WEMPE, P.A., GRIFT, T.E., *et al.*, “Effects of four base cutter blade designs on sugarcane stem cut quality”, *Transactions of the ASABE*, v. 60, n. 5, pp. 1551–1560, 2017. doi: <http://doi.org/10.13031/trans.12345>.
- [18] BORGES, J.F.M., MUGNAINE, M., CAMILO JUNIOR, A., *et al.*, “Ultra high molecular weight polyethylene doped with iron through high energy mechanical alloying”, *Matéria*, v. 25, n. 3, e12791, 2020. doi: <http://doi.org/10.1590/s1517-707620200003.1091>.
- [19] SEO, J., KIM, D.Y., KIM, D.C., *et al.*, “Recent developments and challenges on machining of carbon fiber reinforced polymer composite laminates”, *International Journal of Precision Engineering and Manufacturing*, v. 22, n. 12, pp. 2027–2044, 2021. doi: <http://doi.org/10.1007/s12541-021-00596-w>.
- [20] SHEN, S.-L., CHAI, J.-C., HONG, Z.-S., *et al.*, “Analysis of field performance of embankments on soft clay deposit with and without PVD-improvement”, *Geotextiles and Geomembranes*, v. 23, n. 6, pp. 463–485, 2005. doi: <http://doi.org/10.1016/j.geotextmem.2005.05.002>.
- [21] SAKLESHPUR, V.A., PREZZI, M., SALGADO, R., “Ground engineering using prefabricated vertical drains: a review”, *Geotechnical Engineering*, v. 49, pp. 45–64, 2018.
- [22] DREGER, A.A., BARBOSA, L.A., SANTANA, R.M.C., *et al.*, “Caracterização mecânica e morfológica de solados produzidos com resíduos de laminados de PVC da indústria calçadista”, *Matéria*, v. 23, n. 1, e11952, 2018. doi: <http://doi.org/10.1590/s1517-707620170001.0288>.
- [23] CHRISTIAN, F.B., BIENVENU, K., KHALIFA, M., *et al.*, “Experimental determination of the level of damage suffered by rigid PVC pipes under quasi-static impact load”, *Matéria*, v. 21, n. 1, pp. 83–91, 2016. doi: <http://doi.org/10.1590/S1517-707620160001.0008>.
- [24] DALAGNOL, R.D., FRANCISQUETTI, E.L., SANTANA, R.M.C., “Influence of alternative polymeric plasticizer to DOP in thermal and dynamic-mechanical properties of PVC”, *Matéria*, v. 27, n. 2, e13183, 2022. doi: <http://doi.org/10.1590/s1517-707620220002.1383>.
- [25] XU, H., CHEN, K., “Experimental study on cutting plastic drainage plate by EPB shield machine”, *Journal of Liaoning Technical University*, v. 38, n. 5, pp. 416–423, 2019.
- [26] FENGYUAN, L.I., YANDONG, Y., HUAGUO, X.U., “Key technologies for shield cutting plastic drainage plate in consolidated clay”, *Tunnel Construction*, v. 39, n. 6, pp. 913, 2019.
- [27] LIU, H., CHU, J., “A new type of prefabricated vertical drain with improved properties”, *Geotextiles and Geomembranes*, v. 27, n. 2, pp. 152–155, 2009. doi: <http://doi.org/10.1016/j.geotextmem.2008.09.006>.